MICROBUNCHING WITH A TWIST*

E. Hemsing, P. Musumeci, A. Marinelli and J. B. Rosenzweig
Particle Beam Physics Laboratory, UCLA, Los Angeles, CA 90095, USA

Abstract

An electron beam that is subject to the typical FEL microbunching instability is microbunched longitudinally in both density and velocity, according to the shape of the ponderomotive phase bucket. Higher-order three-dimensional microbunching geometries can be created if the e-beam interacts either with a more complicated resonant field structure, or at higher harmonics of the fundamental resonance. At harmonics inside a helical wiggler, the e-beam interacting with an axisymmetric gaussian laser field becomes microbunched into a helix, or combination of twisted helices, depending on the harmonic number. The twisted e-beam can then be used to emit coherent light with orbital angular momentum in a downstream radiator. An experimental effort to explore the principles of this interaction is discussed.

HELICAL MICROBUNCHING

The helical microbunching of a relativistic electron beam has been studied recently both analytically and in simulation [1]. The motivation for generating such exotic beam distributions comes from the possibility of using them as delicately tunable sources of light that carries orbital angular momentum (OAM) [2, 3, 4]. In addition to the spin momentum carried by light due to the polarization, light can also carry OAM due to an azimuthal component of the photon momentum that is manifest as a helical phase. Pure paraxial EM modes carry $l_i \hbar$ of OAM per photon where l_i is the azimuthal mode number. This type of light, if generated at x-ray wavelength scales obtainable in modern FELs, may serve to expand the suite of exploratory tools available for future research at ultra short wavelengths due to the myriad of potential uses [5].

The principle behind the helical structure of the microbunching lies in the complementary coupling between azimuthal modes in the e-beam and the radiation field at harmonics in a helical undulator. Sasaki and McNulty[6] were the first to realize that the harmonic FEL emission from helical undulators carries OAM. That is, the radiation field emitted from the e-beam at harmonics h above the fundamental has an associated helical phase structure. The e-beam has a purely longitudinal microbunching structure in this case (no azimuthal microbunching modes are excited), but in [1] it was shown this type of interaction can also happen in reverse – that an axisymmetric laser input
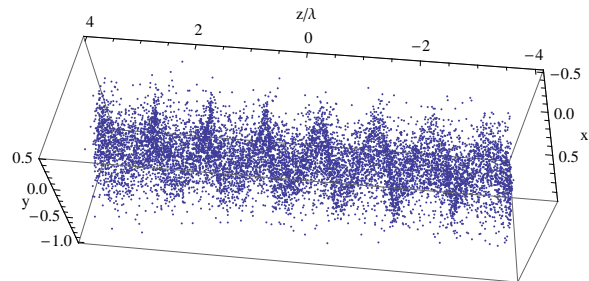
New and Emerging Concepts

Figure 1: Helical electron beam distribution resulting from 3D simulations with code TREDI.

can excite azimuthal modes in the e-beam. The coupling between the field and azimuthal e-beam modes, l, is given by

$$\delta_{l, l_i \pm (h-1)} \tag{1}$$

where h is the harmonic number and + (-) is for a right- (left-) handed undulator polarization. As a result, electron beams with a helical structure can be generated by a simple transversely gaussian input. These beams, once bunched, can then emit superradiant light with OAM in the manner of [3, 4, 7] for FELs or through other radiation processes such as coherent transition radiation[8].

The HELiX (HELical iFEL eXperiment) at the Neptune laboratory at UCLA is designed to explore this concept by generating and measuring helical microbunching of a relativistic electron beam. The 12.5 MeV e-beam interacts at the second harmonic resonance of the combined fields of the Halbach-type helical magnetic undulator and a co-propagating input laser pulse. The input λ=10.6 μm CO_2 laser has a gaussian transverse profile and a > 100 ps pulse length which is much longer than the short <1ps e-beam bunch length. Coupling to the otherwise suppressed harmonic motion in the helical undulator can be accomplished by tightly focusing the input field such that the electrons interact with the transverse gradients of input EM field. If both the e-beam and the laser are coaxial, electrons on opposite sides of a gaussian laser profile are pushed in opposite longitudinal directions and the electrons are rearranged naturally into a spring-like density (and velocity) distribution (See Figure 1)

For helical microbunching it is convenient to define a discrete modal bunching factor of the form

$$b_l = \frac{1}{N} \sum_j^N e^{i\psi_j + i l \phi_j} \tag{2}$$

where N is the number of electrons in the bunch, ψ_j is the position of the jth electron in the ponderomotive phase

bucket and ϕ_j is the azimuthal position. For the HELiX right-handed undulator, the gaussian input laser mode (l=0) at the second harmonic excites a dominant l=−1 mode in the e-beam. For small misalignments or other deviations from the optimum condition, the structure of the 3D microbunching geometry can be gauged by the relative amplitude of microbunching into spatial modes adjacent to the design mode.

In order to quantify the tolerances and limitations on the upcoming experiment, results from numerical simulations are presented in which several characterisitcs of the input laser are varied, and the modal bunching factors $|b_l|$ are calculated. The laser spot size is scanned, the propagation axis is both laterally displaced and tilted with respect to the longitudinal e-beam axis, and the longitudinal position of the laser beam waist inside the undulator is varied. Simulations of the HELiX scheme with a typical Neptunian electron beam were performed with Tredi, a 3D numerical tracking code that has been benchmarked[9]. Ten thousand particles were used to model a 300 pC beam with energy γ=24.73, size σ_x=200 μm, emittance $\epsilon_{N,x}$=6 mm-mrad and slice energy spread σ_γ=10^{-6}. The beam is close to beta-matched for the natural undulator focusing where K_{rms}=0.58. For all simulations the laser field is circularly polarized with P=30 MW of input power. The helical undulator has 12 periods, each with wavelength λ_w =1.9 cm. The undulator entrance is positioned at $z_0 = 0$. The bunching is calculated ∼5 cm past the last magnet in the undulator, the field of which is mapped directly from the RADIA[10] model design. The simulations are therefore a close representation to the actual running scenario.

Spot size – Since the e-beam interacts with the gradients of the input laser field, the spot size of the waist inside the undulator will have an effect on the magnitude of the microbunching into the desired $l = -1$ mode, but should not strongly affect the other modes amplitudes. Naturally, a small laser spot size leads to larger field gradients, and therefore stronger coupling to the harmonic motion. There is a balance, however, between making the spot size small enough to increase the coupling but not so small that the laser field rapidly diffracts away from the e-beam. One must also be careful of the inherent Guoy phase shift of the gaussian beam which shifts the fields $\pi/4$ in phase over one Rayleigh length $\pi w_0^2/\lambda$. Results of the spot size scan are shown in Figure 2 where it is clear that bunching is maximized around w_0=250 μm, but with little over variation over 200-300 μm.

Parallel shift – The symmetry of the designed experiment with both the e-beam and laser coaxial is such that the electrons experience axisymmetric field gradients across the laser profile. A parallel shift of the laser propagation axis breaks this symmetry and results in the excitation of microbunching into adjacent azimuthal modes. Figure 3 shows the magnitude of this effect for shifts up to five times the transverse e-beam rms size, after which the interaction becomes too weak to generate significant bunching. These results suggests that the parallel shift should be <200 μm
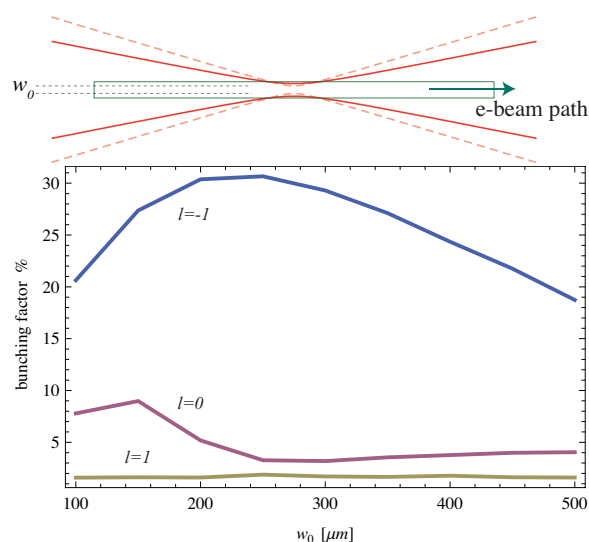

Figure 2: Bunching factor as a function of co-linear laser spot size for three different bunching modes. The waist is held at z_0=10 cm.
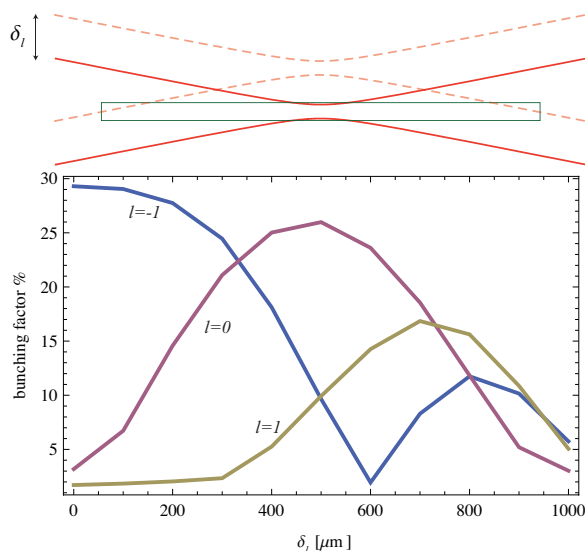

Figure 3: Bunching versus a parallel shift of the laser beam with respect the to e-beam axis. Spot size is w_0= 300 μm.

in order to preserve dominant bunching into the $l = -1$ mode.

Angular misalignment – An angular tilt of the laser propagation axis (rotated about the z_0=10 cm waist position) can also lead to impurities in the microbunching structure. Tilts also change the tuning of the interaction since the effective laser wavelength experienced by the e-beam is lengthened. In Figure 4 the laser is tilted up to 11 mrad. The system was not retuned to accommodate the angles. Strong helical bunching is shown to be preserved through 2 mrad of inclination, which translates to a 500 μm horizontal displacement of the laser over the entire undulator length. This type of misalignment should be straightfor-
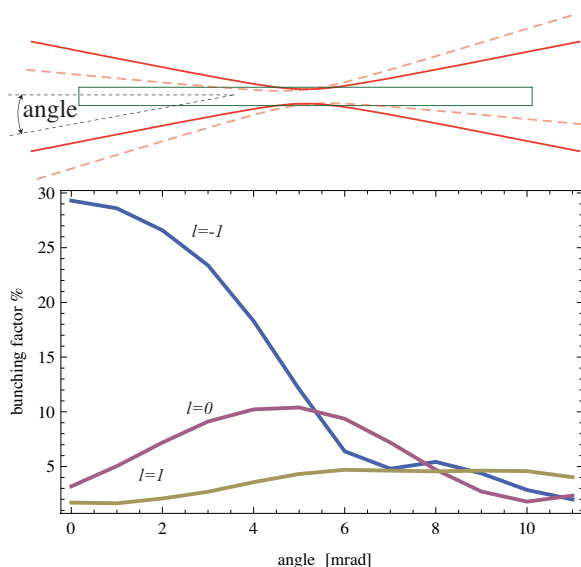
Figure 4: Bunching versus an angular tilt of the laser beam in the x-plane with the z_0=10 cm waist as a fulcrum. Spot size is w_0= 300 μm.
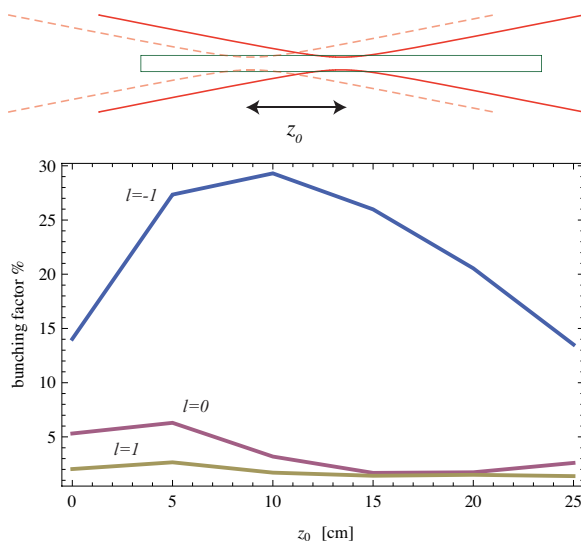

Figure 5: Bunching versus waist position for a spot size of w_0= 300 μm.

ward to avoid provided sufficiently accurate knowledge of the electron trajectory inside the undulator.

Laser waist position – The longitudinal position of the waist along the interaction can also effect the magnitude of the bunching at the exit. Varying this parameter, like the spot size, does not have a strong effect on the bunching into other modes. Figure 5 demonstrates that, for a w_0= 300 μm spot size, the z_0=10 cm waist positioning is optimal.

Interferometry – Since the structure of the microbunched beam obviously cannot be verified by direct observation, the telling signature of the helical geometry is emission of light with a helical phase. One of the simplest methods to extract the microbunching characteristics is through co-

herent transition radiation[11, 12, 13]. CTR from the the helically microbunched beam is also predicted to have a helical phase geometry as well as a modified angular distribution and total energy[8]. In principle, these features could be measured to distinguish between different helical modes radiating coherently in the beam. Experimentally however, systematic fluctuations in charge, laser power and bunch length limit the ability to resolve the small differences in the emission. Further, the total calculated CTR energy is on the order of 100 pJ, which limits possible detection schemes at 10.6 μm and specifically prevents resolution of the transverse radiation profile with available detectors. This precludes use of certain elegant mode-sorting devices[14] to detect the phase content since only the total energy of the CTR pulse can be measured with the liquid nitrogen cooled HgCdTe detector. The scenario is further complicated by the characteristic radial field polarization of the CTR.

To resolve these issues and discern the dominant microbunching mode, a modified version of the OAM mode selector in [14] has been designed and built. Shown schematically in Figure 7, this modified Michaelson interferometer uses an extra bounce in one leg to flip the azimuthal mode number of the CTR from $l = -1$ to $l = 1$. This also flips the phase in the horizontal polarization such that when the radially polarized CTR signal interferes with the mirror image of itself, the total power signal focused into the detector is proportional to

$$P_{CTR} \propto 2 + \delta_{l,\pm 1} \cos 2\alpha. \tag{3}$$

where α is the phase delay shown in Figure 7. The design beam with the helical phase will therefore produce a sinusoidal power signal as a function of the delay, whereas a beam with an $l = 0$ purely longitudinal microbunching structure will generate a constant signal. This behavior is specific to the radially polarized light of CTR, and will allow direct verification of the mode content in the beam. Recent simulations with the code QUINDI[15] to calculate the far-field CTR from the helical beam have confirmed both the imbedded helical phase front (Figure 6) and the ability of the interferometer to distinguish between the scenarios.

CONCLUSIONS

Simulations confirm analytic predictions of dominant helical microbunching and indicate that the effect can be maximized for the design $l = -1$ mode with a laser spot size of $w_0 \simeq 200$-300 μm located z_0=10 cm inside the entrance of the undulator. The tolerances on the lateral and angular positioning, set by the desire to preserve the dominance and purity of the mode, suggest a transverse alignment precision of within $|\delta_l|$ <200 μm for a parallel offset and <2 mrad in angle. A new interferometer device has been built for the recovering the helical phase in the emitted CTR as described in [8] and confirmed through simulation.
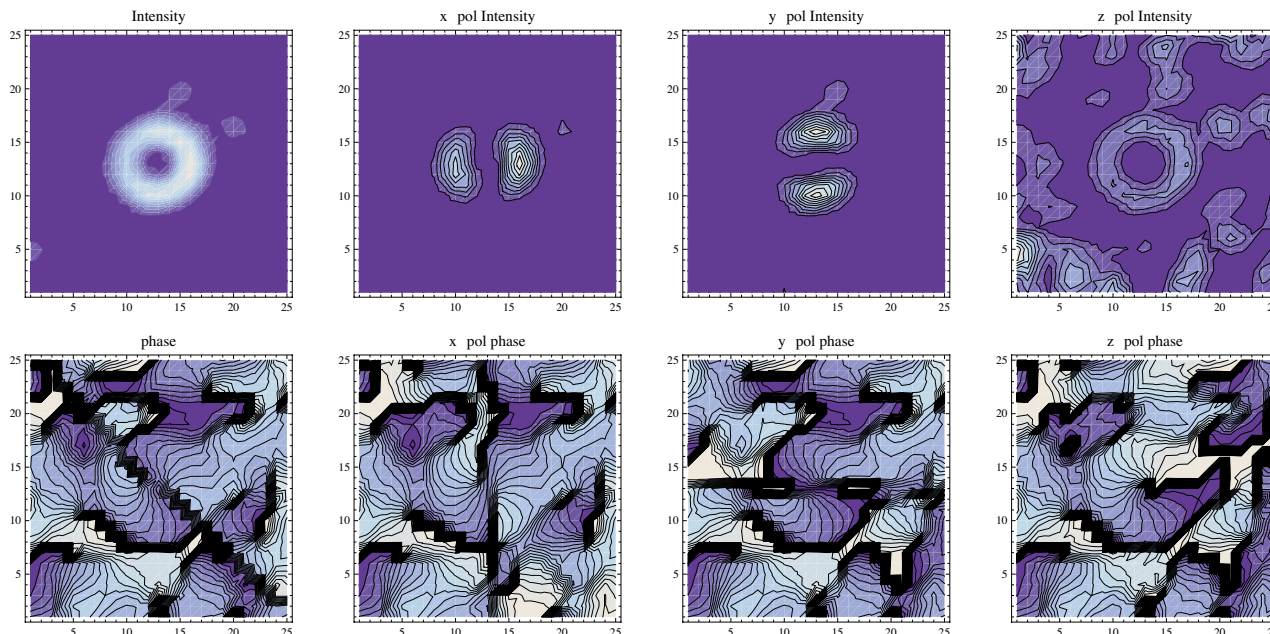
Figure 6: Intensity and phase CTR profile distributions from QUINDI simulations of an $l = -1$ beam. Note the transverse polarizations have an $l = -1$ helical phase superimposed on a π phase shift due to the radial polarization. There is no such shift in the much smaller z component, the phase of which closely represents that of the e-beam structure.
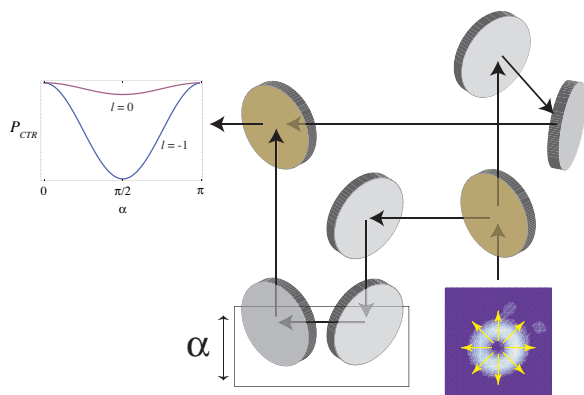

Figure 7: Interferometer for resolving helical phase of CTR and the discriminating power signal.

References

[1] E. Hemsing, P. Musumeci, S. Reiche, R. Tikhoplav, A. Marinelli, J. B. Rosenzweig, and A. Gover, Physical Review Letters **102**, 174801 (2009).

[2] L. Allen, M. W. Beijersbergen, R. J. C. Spreeuw, and J. P. Woerdman, Phys. Rev. A **45**, 8185 (1992).

[3] E. Hemsing, A. Gover, and J. Rosenzweig, Physical Review A **77**, 063831 (2008).

[4] E. Hemsing, A. Marinelli, S. Reiche, and J. Rosenzweig, Phys. Rev. ST Accel. Beams **11**, 070704 (2008).

[5] L. Allen, S. M. Barnett, and M. J. Padgett, *Optical angular momentum* (Institute of Physics Pub., 2003), ISBN 0750309016.

[6] S. Sasaki and I. McNulty, Phys. Rev. Lett. **100**, 124801 (2008).

[7] E. Hemsing, J. B. Rosenzweig, and A. Gover, in *Proceedings of the 30th International Free Electron Laser Conference.* (2008), pp. 167–171.

[8] E. Hemsing and J. B. Rosenzweig, Journal of Applied Physics **105**, 093101 (pages 6) (2009).

[9] L. Giannessi, P. Musumeci, and M. Quattromini, Nucl. Instrum. Methods Phys. Res., Sect. A **436**, 443 (1999).

[10] http://www.esrf.eu/Accelerators/Groups /InsertionDevices/Software/Radia.

[11] A. Tremaine et al, Phys. Rev. Lett. **81**, 5816 (1998).

[12] A. H. Lumpkin et al, Phys. Rev. Lett. **86**, 79 (2001).

[13] S. Y. Tochitsky et al, Phys. Rev. ST Accel. Beams **12**, 050703 (2009).

[14] J. Leach, M. J. Padgett, S. M. Barnett, S. Franke-Arnold, and J. Courtial, Phys. Rev. Lett. **88**, 257901 (2002).

[15] D. Schiller, S. Reiche, and M. Ruelas, in *Particle Accelerator Conference, 2007. PAC. IEEE* (2007), pp. 3612–3614.